International Journal of Nanomedicine

Dovepress
open access to scientific and medical research

Open Access Full Text Article

ORIGINAL RESEARCH

Novel T7-Modified pH-Responsive Targeted Nanosystem for Co-Delivery of Docetaxel and Curcumin in the Treatment of Esophageal Cancer

This article was published in the following Dove Press journal:
International Journal of Nanomedicine

Lian Deng[1,*]
Xiongjie Zhu[1,*]
Zhongjian Yu[1]
Ying Li[1]
Lingyu Qin[1]
Zhile Liu[1]
Longbao Feng[2]
Rui Guo[2]
Yanfang Zheng[1]

[1]Department of Oncology, Zhujiang Hospital of Southern Medical University, Guangzhou 510282, China; [2]Key Laboratory of Biomaterials of Guangdong Higher Education Institutes, Guangdong Provincial Engineering and Technological Research Center for Drug Carrier Development, Department of Biomedical Engineering, Jinan University, Guangzhou 510632, China

*These authors contributed equally to this work

Background: Although single-drug chemotherapy is still an effective treatment for esophageal cancer, its long-term application is limited by severe side-effects, poor bioavailability, and drug-resistance. Increasing attention has been paid to nanomedicines because of their good biological safety, targeting capabilities, and high-efficiency loading of multiple drugs. Herein, we have developed a novel T7 peptide-modified pH-responsive targeting nanosystem co-loaded with docetaxel and curcumin for the treatment of esophageal cancer.

Methods: Firstly, CM-β-CD-PEI-PEG-T7/DTX/CUR (T7-NP-DC) was synthesized by the double emulsion (W/O/W) method. The targeting capacity of the nanocarrier was then investigated by in vitro and in vivo assays using targeted (T7-NP) and non-targeted nanoparticles (NP). Furthermore, the anti-tumor efficacy of T7-NP-DC was studied using esophageal cancer cells (KYSE150 and KYSE510) and a KYSE150 xenograft tumor model.

Results: T7-NP-DC was synthesized successfully and its diameter was determined to be about 100 nm by transmission electron microscopy and dynamic light scattering. T7-NP-DC with docetaxel and curcumin loading of 10% and 6.1%, respectively, had good colloidal stability and exhibited pH-responsive drug release. Good biosafety was observed, even when the concentration was as high as 800 μg/mL. Significant enhancement of T7-NP uptake was observed 6 hours after intravenous injection compared with NP. In addition, the therapeutic efficacy of T7-NP-DC was better than NP-DC and docetaxel in terms of growth suppression in the KYSE150 esophageal cancer model.

Conclusion: The findings demonstrated that T7-NP-DC is a promising, non-toxic, and controllable nanoparticle that is capable of simultaneous delivery of the chemotherapy drug, docetaxel, and the Chinese Medicine, curcumin, for treatment of esophageal cancer. This novel T7-modified targeting nanosystem releases loaded drugs when exposed to the acidic microenvironment of the tumor and exerts a synergistic anti-tumor effect. The data indicate that the nanomaterials can safely exert synergistic anti-tumor effects and provide an excellent therapeutic platform for combination therapy of esophageal cancer.

Keywords: nanocarrier, T7 peptide, pH-responsive, docetaxel, esophageal cancer

Introduction

Esophageal cancer is the seventh most common cancer and ranks sixth in terms of cancer-related mortality worldwide. It has been estimated that around 572,000 cases led to 508,000 deaths in 2018.[1] Although continuous scientific progress has benefited cancer patients, those with advanced lung cancer still suffer from the deficiencies of chemotherapy, which are mainly attributed to poor tumor targeting, high

Correspondence: Yanfang Zheng; Rui Guo
Tel +86 18665000236
Email 18665000236@163.com; guorui@jnu.edu.cn

submit your manuscript | www.dovepress.com
DovePress
http://doi.org/10.2147/IJN.S257312

toxicity and side effects, short half-life, uncontrolled release, poor bioavailability, and drug resistance.[2,3]

Among the commonly used chemotherapeutic agents, taxanes are a class of drugs used in advanced lung cancer and have long-lasting anti-cancer properties.[4] Of these, docetaxel (DTX) is a second generation drug in the paclitaxel family that has demonstrated promising survival benefits in esophageal cancer patients.[5] Unfortunately, single chemotherapeutic drugs have limitations and side-effects that lead to lower patient compliance.[6] In order to improve the efficacy of chemotherapeutic drugs and reduce their side-effects, some proprietary Chinese medicines are often added as adjuvant drugs in clinical applications. Among them, curcumin (CUR) is the most representative. As reported in the literature,[7,8] curcumin, a natural polyphenolic compound derived from the roots of turmeric, has anti-inflammatory and anti-tumor effects, and is chemosensitizing. In a Phase I clinical study of curcumin plus docetaxel in patients with advanced breast cancer, better therapeutic efficacy was observed in eight of 14 patients compared with single docetaxel therapy.[9] In addition, in other studies in ovarian, prostate, and breast cancer, curcumin combined with docetaxel was found to be more effective than docetaxel alone.[10–12] Based on these previous studies, we speculate that the combination of curcumin and docetaxel has potential in the treatment of esophageal cancer.

In past decades, the inherent limitations of traditional cancer therapy have led to the development and application of various nanotechnologies to treat cancer more effectively and safely.[13,14] The increasing interest in nanotechnology for cancer is due to its unique and attractive features, such as its utility for drug delivery, diagnosis, imaging, and synthetic vaccine development, as well as the inherent therapeutic properties of some nanomaterials.[15–17] To precisely control the release of drug at the tumor site and to meet requirements for increased anti-tumor effect and reduced damage to normal tissues, research has made great contributions in the area of stimuli-responsive release of materials (for example, pH, redox state, and enzymes).[18–20] Based on the characteristic acidity of the tumor microenvironment, Li et al[21] developed pH-responsive nanoparticles that improved the anti-tumor effect of paclitaxel on drug-resistant and metastatic breast cancer. Similarly, another study on pH-responsive nanocarriers also confirmed their capability for drug-release on demand to better inhibit the activity of HeLa cells.[22] In addition, poor permeability of tumors to drugs is a major obstacle to cancer treatment. Targeted delivery of nanomedicines to tumor cells could enhance tumor detection and therapy. Very recently, Gao[23] demonstrated that tumor penetration of nanoparticles modified with T7 peptide was 7.89-fold higher compared with unmodified nanoparticles. Jiang et al[24] confirmed that T7-modified nanoparticles showed more pronounced accumulation in the tumor and a better curative effect compared with unmodified nanoparticles.

At present, most nanomedicine research is focused on single-drug treatment of cancer, which can benefit patients to a certain extent by, for example, reducing toxicity. However, administration of nanomedicines in combination with traditional clinical therapies, such as radiation, small molecule, and biological drugs, will have the greatest impact. It has previously been demonstrated that co-administration of curcumin with docetaxel via a nanocarrier had the potential to improve anti-tumor efficacy in breast cancer.[12] Furthermore, in a Phase III TRIAL in patients with acute myeloid leukemia, Veyons, a liposomal nanomedicine for co-delivery of cytarabine and daunorubicin, prolonged life by 6–10 months compared with standard treatment.[25] Therefore, the synergistic antitumor effect of docetaxel and curcumin in esophageal cancer may be enhanced by nanocarrier delivery.

With regard to the potential of nanomedicine for combination therapy, in the present research we report a novel T7-targeting nanosystem for co-delivery of docetaxel and curcumin with pH-responsive drug-release capability (T7-NP-DC). The stimuli-responsive release, cytotoxicity, cellular uptake, and permeability in 3D tumorspheres of T7-NP-DC were thoroughly investigated in vitro and in vivo. According to the results, the synthesized nanomedicine not only exhibits good tumor targeting, but also has a good anti-tumor effect, which shows potential for accurate treatment of tumors in the future.

Materials

Fetal bovine serum (FBS), 1640 culture medium, and Dulbecco's modified Eagle's medium (DMEM) were obtained from Life Technologies Inc. (Gibco-BRL, Gaithersburg, MD, USA). Docetaxel and curcumin were purchased from Yuanye Corporation (Shanghai, China) and Ronghe Pharmaceutical Technology Development Co., Ltd. (Shanghai, China), respectively. α-Maleimidyl-ω-N-hydroxysuccinimidyl polyethylene glycol (NHS-PEG-MAL, MW 3500) was obtained from Jenkem Technology (Beijing, China). T7

polypeptide (SH-CHAIYPRH) was purchased from Jill Biochemical Co., Ltd. (Shanghai, China). Transferrin receptor (TfR) primary antibody was purchased from eBioscience (Waltham, MA, USA). Cell Counting Kit-8 (CCK-8) was purchased from the Beyotime Institute of Biotechnology (Shanghai, China). Dimethyl sulfoxide (DMSO), methanol, and branched polyethyleneimine (PEI) with an average molecular weight of 1.8 kDa were purchased from Aladdin Biochemical Technology (Shanghai, China). LysoTracker was bought from Meilun Biotechnology Co., Ltd. (Dalian, China). Annexin V-FITC/PI apoptosis detection kit was purchased from Kaiji Biotechnology Co., Ltd. (Nanjing, China). Nude mice, bedding, and feed were purchased from the experimental animal center of Southern Medical University (Guangzhou, China).

Methods

Preparation and Characterization of Nanoparticles

Synthesis of CM-β-CD

CM-β-CD was synthesized as follows: β-cyclodextrin (β-CD, 2.14 g) and NaOH (0.3 g) were dissolved in water (30 mL) and treated with 1% (w/w) aqueous monochloroacetic acid (5 mL). The mixture was stirred at 50°C for 4 hours and then the pH was adjusted to 7 with hydrochloric acid. Excess ethanol was added to the neutral solution, producing a white precipitate. The solid precipitate was filtered and dried under vacuum to give carboxymethylated β-CD (CM-β-CD).

Synthesis of CM-β-CD-PEI

CM-β-CD (1.2 g) was activated with carbonyldiimidazole (CDI, 0.36 g) in DMSO (5 mL) at room temperature for 2 hours. Polyethyleneimine (100 mg) was added dropwise to the activated CM-β-CD solution and stirred at room temperature for 12 hours. The mixture was purified by dialysis against water (MW 1000 Da) for 7 days followed by lyophilization to give CM-β-CD-PEI.

Synthesis of CM-β-CD-PEI-PEG

CM-β-CD-PEI (1 g) and MAL-PEG-NHS (1 g) were dissolved in water (10 mL) in an ampule, followed by addition of saturated aqueous $NaHCO_3$ to adjust to pH 7.5–8.5. The mixture was then stirred at room temperature. After 4 hours, the mixture was purified by dialysis against water (MW 1000 Da) for 24 hours followed by lyophilization to give a lavender solid.

Synthesis of CM-β-CD-PEI-PEG-T7

To conjugate CM-β-CD-PEI-PEG to T7, CM-β-CD-PEI-PEG (0.25 g) was dissolved in water (5 mL). T7 polypeptide solution (1 mL) was added and the pH was adjusted to 6.0–6.5. The reaction mixture was stirred at room temperature for 24 hours, after which the Mal group of CM-β-CD-PEI-PEG had reacted with the thiol group of Cys-T7. Finally, the conjugate CM-β-CD-PEI-PEG-T7 was obtained by dialysis and lyophilization.

Synthesis of CM-β-CD-PEI-PEG-T7/DTX/CUR

CM-β-CD-PEI-PEG-T7/DTX/CUR was synthesized by the double emulsion (W/O/W) method. Briefly, CM-β-CD-PEI-PEG-T7 (40 mg) was dissolved in ethyl acetate (1 mL) followed by addition of docetaxel and curcumin solutions (1 mL). The mixture was emulsified by sonication (150 W, 60 seconds) to form a colloidal solution. A 4% PVA solution (2 mL) was then added to the colloidal solution and the mixture was sonicated (150 W, 90 seconds) to form a W/O/W double emulsion. After 4 hours, CM-β-CD-PEI-PEG-T7/DTX/CUR was obtained by centrifugation at 5600×g for 10 minutes at room temperature and washing twice with distilled water. CM-β-CD-PEI-PEG-T7/DTX and CM-β-CD-PEI-PEG-T7/CUR were prepared using the aforementioned method. The concentrations of DTX and CUR were measured by ultraviolet spectrophotometry. Drug-loading (DL) content and encapsulation efficiency (EE) were calculated as follows:

$$EE\ (\%)=A_1/A_2\times 100\%$$

$$DL\ (\%)=A_1/B\times 100\%$$

A_1 is the weight of drug in the carrier material, A_2 is the weight of drug added, and B is the weight of carrier material.

^{1}H NMR

The chemical structures of CM-β-CD-PEI-PEG-T7 and CM-β-CD-PEI-PEG were characterized by ^{1}H nuclear magnetic resonance (NMR) spectroscopy (300 MHz, Varian, USA) using D_2O as the solvent.

Particle Size Distribution and Morphological Characterization

The particle sizes of CM-β-CD-PEI-PEG-T7/DTX/CUR and CM-β-CD-PEI-PEG-T7 were measured using a Zetasizer Nano ZS (Malvern) apparatus. Briefly, a 1 mg/mL sample (1 mL) was placed in a sample cell and the particle size was measured using a dynamic light

scattering (DLS) laser nanoparticle analyzer at 25°C. The morphologies of CM-β-CD-PEI-PEG-T7/DTX/CUR and CM-β-CD-PEI-PEG-T7 were characterized using transmission electron microscopy (JEOL TEM-1210).

Drug Release

In vitro release of DTX and CUR from CM-β-CD-PEI-PEG-T7/DTX/CUR was studied using the dialysis membrane diffusion technique. Briefly, CM-β-CD-PEI-PEG-T7 /DTX/CUR solution (1 mg/mL, 3 mL) was enclosed in a dialysis bag and placed in phosphate buffer (10 mL, pH 5.5 or 7.4) containing 10% Tween 80 at 37°C. At a predetermined time point, a sample of the buffer (1 mL) was taken for UV-visible spectroscopy and replaced with an equal volume of fresh buffer. The cumulative release of DTX and CUR was calculated as follows:

Percentage release (%)=$M_1/M_0\times100\%$

where M_1 is the mass of released drug and M_0 is the mass of total drug in the nanosystem.

Cell Culture

The non-neoplastic esophageal epithelial cell line, Het-1a, and four esophageal squamous cell carcinoma (ESCC) cell lines, KYSE150, KYSE510, Eca9706, and CaES-17, were donated by Clinical Research Central at Nanfang Hospital, and the study had the approval of the ethical committee of Zhujiang hospital of Southern Medical University in Guangzhou, China. Among them, CaES-17 cells were authenticated by STR profile. Het-1a cells were cultured in DMEM containing 10% FBS and 1% penicillin/streptomycin (all from Gibco, Life Technologies, CA, USA). The four ESCC cell lines were cultured in RPMI 1640 (Gibco, Life Technologies) supplemented with 10% FBS and 1% penicillin/streptomycin at 37°C in a humidified atmosphere containing 5% CO_2.

RNA Extraction and Quantitative Polymerase Chain Reaction (qPCR)

Total RNA was extracted using Trizol reagent according to the manufacturer's (TaKaRa Bio Inc., Japan) instructions. The RNA purity and concentration were evaluated by spectrophotometry using a nanodrop 2000c instrument (Thermo Scientific, Rockford, IL, USA) and reverse transcription was conducted using PrimeScript™ RT Master Mix (TaKaRa Bio Inc., Japan). For TfR quantification, qPCR was performed using TB Green® Premix Ex TaqTM II reagent (TaKaRa Bio Inc., Japan) on a LightCycler 480 system (Roche, Basel, Switzerland).[26] The sequences of the primers were as follows: TfR forward,5′-CTGCCTCTTTCCTGTTGTTGT-3′ and reverse,5′-CTTTGGCCAA AATTTGGCAGC-3′.

Examination of TfR Expression by Flow Cytometry

Cells (Het-1a, KYSE150, KYSE510, CaES-17, and Eca9706) in good condition were digested with trypsin, centrifuged, and then washed three times with phosphate buffered saline (PBS) to remove residual medium. Subsequently, FITC-labeled primary antibody (TfR, 5 μL) was added in the dark to bind with TfR on the cell surface. After 30 minutes, flow cytometry was used to determine the fluorescence intensity of the cells.

Synergistic Effects of Docetaxel and Curcumin

The synergistic effects of different concentrations of docetaxel and curcumin were evaluated by MTT assay. Cells were seeded in 96-well plates (KYSE150 4×10^3/well, KYSE510 3.5×10^3/well) and incubated overnight. The culture medium was replaced with fresh medium (100 μL) containing either single-drug (docetaxel or curcumin) or a combination of the two drugs at various ratios (DTX: CUR 2:1, 1:1, or 1:2). The DTX concentrations in KYSE150 cells were 0, 0.25, 0.5, 1, 2, 4, 8, 16, and 32 ng/mL, and in KYSE510 cells were 0, 0.0625, 0.125, 0.25, 0.5, 1, 2, 4, and 8 ng/mL. After incubation for 48 hours, cell viability was evaluated by MTT assay. The culture medium was removed and the wells treated with MTT solution (20 μL, 5 mg/mL) and 1640 medium (200 μL) without FBS for 4 hours at 37°C. The MTT solution was discarded and DMSO (150 μL/well) was added to dissolve the formazan dye. The absorbance was measured by spectrophotometry at 570 nm. Cell viability and inhibitory effects were determined from the OD values. The combination index (CI) was evaluated using CompuSyn software (Version 1.0), where CI=1 indicated an additive effect, CI>1 indicated an antagonistic effect, and CI<1 indicated a synergistic effect.

Cellular Uptake

A confocal laser scanning microscope (CLSM) was used to evaluate uptake of the nanocarriers. KYSE510 cells were incubated in a confocal culture dish overnight, pretreated with T7 or transferrin (Tf), and then treated with

FITC-labeled NP andT7-NP (200 μg/mL). After incubation for 4 hours, the culture medium was discarded and the cells washed three times with PBS. The cells were fixed with 4% paraformaldehyde for 30 minutes. The paraformaldehyde was then discarded and the cells washed with PBS. Finally, the cells were stained with Hoechst solution for 15 minutes, washed three times, and then the fluorescence intensity was observed by CLSM.

In vitro Cytotoxicity of Nanomedicines

The experimental procedures were the same as those just described, except that the added drug was replaced by the nanomedicines.

Cell Apoptosis

To evaluate the effect of different formulations on apoptosis, cells (KYSE150 and KYSE510) were seeded in 6-well plates at a density of 3×10^5 cells/well for 24 hours and then treated with mixtures containing equivalent DTX concentrations (2 ng/mL) for 48 hours. The cells were washed twice with PBS, subjected to trypsin digestion, and then stained with an Annexin V-FITC/PI apoptosis detection kit (Dojindo, Japan) according to the manufacturer's instructions. Analysis was conducted by flow cytometry.

3-Dimensional Tumorsphere

KYSE510 cells in good condition were digested, resuspended, and then added at a concentration of 1×10^4/mL to a 96-well plate containing 2% agarose. A tumorsphere was formed on the surface after 3 days culture. Following treatment with different formulations, the diameters of the tumorspheres were measured by optical microscopy at days 1, 3, 5, and 7. The following formulas were used for analysis:

$V=\pi*dmax*dmin/6$

Tumorsphere rate of change $(R)=Vi/V0\times100\%$

where Vi represents the volume on day i and

V0 represents the volume on day 0.

Biodistribution of Nanoparticles in vivo

To investigate the biodistribution of nanoparticles in vivo, xenograft-bearing mice were divided into four groups (n=3; NP, NP-DC, T7-NP-D, and T7–NP–DC). The Cy5.5-labeled nanoparticles were injected intravenously and then the fluorescence distribution in mice was observed at 2 and 8 hours using an in vivo live imaging instrument.

In vivo Anti-Tumor Efficacy

Male Balb/c mice (4–5 weeks, 18–20 g) were purchased from the Animal Center of Nanfang Medical University and reared in the SPF region. Cells (1×10^6) in PBS (0.1 mL) were injected subcutaneously into the right flank of the mice. The xenograft-bearing mice were then divided into six groups (PBS, DTX, NP-D, NP-DC, T7-NP-D, and T7-NP-DC), and the drugs were injected intravenously every other day for a total of 12 days. Tumor volumes were monitored by vernier caliper every 3 days and calculated as follows: $length\times width^2/2$.

Biosafety in vivo

Mice were euthanized at the end of the treatment and blood was collected for routine testing, and liver and kidney function tests. The major organs (heart, liver, spleen, lung, and kidney) and tumor were harvested and fixed in 4% paraformaldehyde. Hematoxylin-eosin (HE) staining and immunohistochemistry (IHC) were performed to evaluate the biosafety of the materials and tumor inhibitory effect (Ki-67).

Statistical Analysis

Statistical analysis was conducted using SPSS 20 software. A one-way ANOVA test was used to compare multiple groups. P-values<0.05 were considered statistically significant.

Results

TfR Expression in ESCC and Het-1a Cell Lines

As reported in the literature,[27] TfR is overexpressed in malignant tumors. Herein, the qPCR analysis was performed to measure expression of TfR mRNA in ESCC cell lines and the non-neoplastic esophagus cell line, Het-1a. An increase of TfR mRNA expression was found in ESCC cell lines (KYSE150, KYSE510, Eca9706, and CaES-17) compared to Het-1a (Supplementary Figure S1A, $*P<0.05$, $***P<0.005$). Investigation of TfR expression by flow cytometry, as shown in Supplementary Figures S1B and S1C, revealed that CaES-17 cells had the highest TfR expression, while expression by KYSE150 and KYSE510 cells was also higher than Het-1a cells. In view of the high expression of TfR in malignant tumors, Zhao[28] developed a Tf-decorated nanocarrier that exhibited impressive anti-tumor activity and more efficient cellular uptake in TfR-overexpressing lung cancer cells. Other studies also demonstrated the impressive

uptake efficiency and anti-tumor effect on lung cancer cells.[29,30] We therefore speculated that we could exploit this phenomenon by designing a nanocarrier to specifically bind surface TfR and target tumors.

Inhibitory Effect of Different Formulations in vitro

Adjuvants are often used in the clinic to ameliorate the side-effects of single-drug treatment. Moreover, it has been reported that chemotherapy-sensitizing drugs can be used in combination with a single-drug to enhance anti-tumor activity, suggesting that patients could benefit from combination therapy. Therefore, in this study, we attempted to optimize the formulation of docetaxel and curcumin, using CompuSyn software to calculate the combination index. Firstly, the cells (KYSE150 and KYSE510) in good condition were cultured in 96-well plates and divided into three groups (DTX:CUR 2:1, 1:1, and 1:2). Then, the different formulations of docetaxel and curcumin were added on schedule. The CCK-8 assay was performed 48 hours post-treatment to evaluate inhibition and synergistic anti-tumor efficacy. As shown in Figure 1A–D, in the two cancer cell lines (KYSE150 and KYSE 510), the CI was less than 1 when the DTX:CUR ratio was 1:2. When the DTX:CUR ratio was 2:1 or 1:1, the higher proportion of docetaxel led to weaker synergy, possibly even an antagonistic effect (Table 1 and Supplementary Table S1). Meanwhile, we observed a lower IC_{50} in the T7-NP-DTX/CUR group, compared with the other group (Supplementary Table S2). Consistent with previous studies, it was found that the combined application of curcumin and docetaxel could indeed synergistically enhance

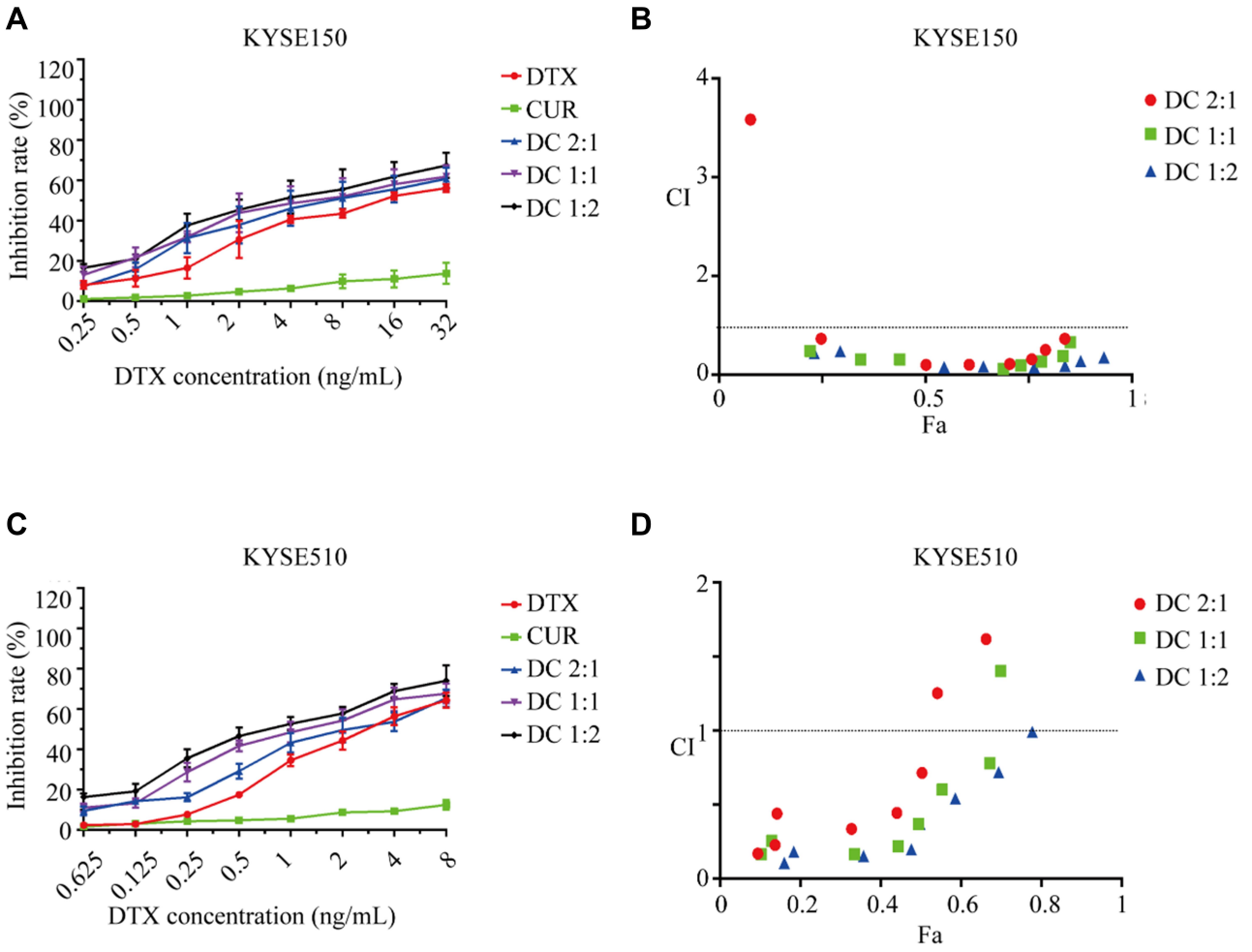

Figure 1 Demonstration of optimal formulations in ESCC. Following treatment with different formulations (DTX:CUR=2:1, 1:1, and 1:2), inhibition efficacy of KYSE150 was measured by CCK-8 assay (**A**), and then the synergistic effect was further evaluated by the combination index (CI) (**B**), and further examination of KYSE510 inhibition efficacy was measured by CCK-8 assay (**C**) and evaluated by the combination index (CI) (**D**).

Table 1 Combination Index (CI) of Different Drug Formulations in KYSE150

DTX (ng/mL)	DTX:CUR 2:1	DTX:CUR 1:1	DTX:CUR 1:2
	CI CI CI		
0.25	5.17357	0.48132	0.43564
0.5	0.73178	0.31493	0.47814
1	0.20394	0.31295	0.15368
2	0.20896	0.12393	0.1687
4	0.22412	0.18779	0.15239
8	0.31678	0.27078	0.18287
16	0.50756	0.37689	0.27741
32	0.73219	0.66478	0.35483

the antitumor effect.[11,12] Hence, we finally determined that DTX:CUR(1:2) was the optimal formulation for synergistic anti-tumor activity against esophageal cancer.

Synthesis of CM-β-CD-PEI and CM-β-CD -PEI-PEG-T7

The synthesis of CM-β-CD-PEI-PEG-T7 is shown in Scheme 1 drawn by ourselves. First, β-cyclodextrin reacted with chloroacetic acid under basic conditions to form carboxymethyl-β-cyclodextrin (CM-β-CD). CM-β-CD-PEI was synthesized by amidation reaction of CM-β-CD and polyethyleneimine. Reaction of the product with MAL-PEG-NHS, a coupling agent, gave CM-β-CD-PEI-PEG. The chemical structure of CM-β-CD-PEI-PEG was characterized by nuclear magnetic resonance spectroscopy (^{1}H NMR), as shown in Supplementary Figure S2. As planned, T7 was combined with CM-β-CD-PEI via NHS-PEG-MAL to construct the drug nanocarrier (CM-β-CD-PEI-PEG-T7). The NMR spectrum contained a D_2O solvent peak at 4.7 ppm; proton absorption peaks at chemical shift values of 3.724 and 3.822 ppm were attributed to characteristic peaks of the T7 peptide in CM-β-CD -PEI-PEG-T7; the proton absorption peaks at chemical shifts of 5.0 and 3.2–3.6 ppm were attributed to β-CD. Together, the successful synthesis of CM-β-CD-PEI-PEG-T7 was demonstrated by ^{1}H NMR.

Characterization of Drug-Loaded Nanoparticles

According to previous studies,[31] nanoparticle size can affect their excretion pathway in vivo and their ability to enter cells. It is therefore necessary to characterize the nanomedicines. The regular spherical shape of CM-β-CD-PEI-PEG-T7 before and after drug loading was scanned by transmission electron microscopy (TEM) (Figure 2A). Many small particles appeared in the nanospheres after drug loading, which was attributed to the loading of docetaxel and curcumin (Figure 2A). Subsequently, dynamic light scattering (DLS) was performed to characterize the obtained nanoparticles (Figure 2B). The particle size of CM-β-CD-PEI-PEG -T7 was 228.35±4.59 nm. The diameter of the nanocarrier increased to 312.74±6.57 nm after loading of docetaxel and curcumin, which was consistent with the results from TEM. Meanwhile, we further discuss the polydispersity index (PdI) results of developed formulation (CM-β-CD-PEI-PEG-T7: PDI=0.53, CM-β-CD-PEI-PEG-T7-DTX/CUR: PDI=0.38).

Stimuli-Responsive (pH) Drug-Release in vitro

Stimuli-responsive release of nanomedicines is based on the specific microenvironment of tumor tissue, which not only enables maximum release of drug into tumor tissue, but also reduces damage to normal tissue.[32] Herein, we tested the drug-release efficiency of the nanomedicines in a simulated tumor microenvironment. The DTX and CUR content were measured at 10% and 6.1%, respectively, using HPLC and UV spectroscopy. Normal physiological and tumor microenvironment states were simulated using PBS and a pH 5.5 solution, respectively. As shown in Supplementary Figure S3, the drug-release rates were significantly enhanced in the slightly acidic environment, and the cumulative release rates of DTX and CUR reached 86.8% and 60.2%, respectively. In contrast, in PBS alone, the cumulative release rate of DTX was decreased to 26.5%, and that of CUR was 12.3%. In previous research, the DTX-loading content of PCL-PEG reached 10.4% and almost 90% DTX was released at pH 5.5 after 24 hours, which is similar to our results.[33] It is apparent that our materials also have a good drug loading rate.

Cytotoxicity in vitro

To further explore the anti-tumor efficacy of the nanomedicines in vitro, we treated esophageal cancer cells (KYSE150 and KYSE510) with different formulations and determined cell viability using the CCK-8 assay (Figure 3C and Supplementary Figure S6C), apoptosis rate by flow

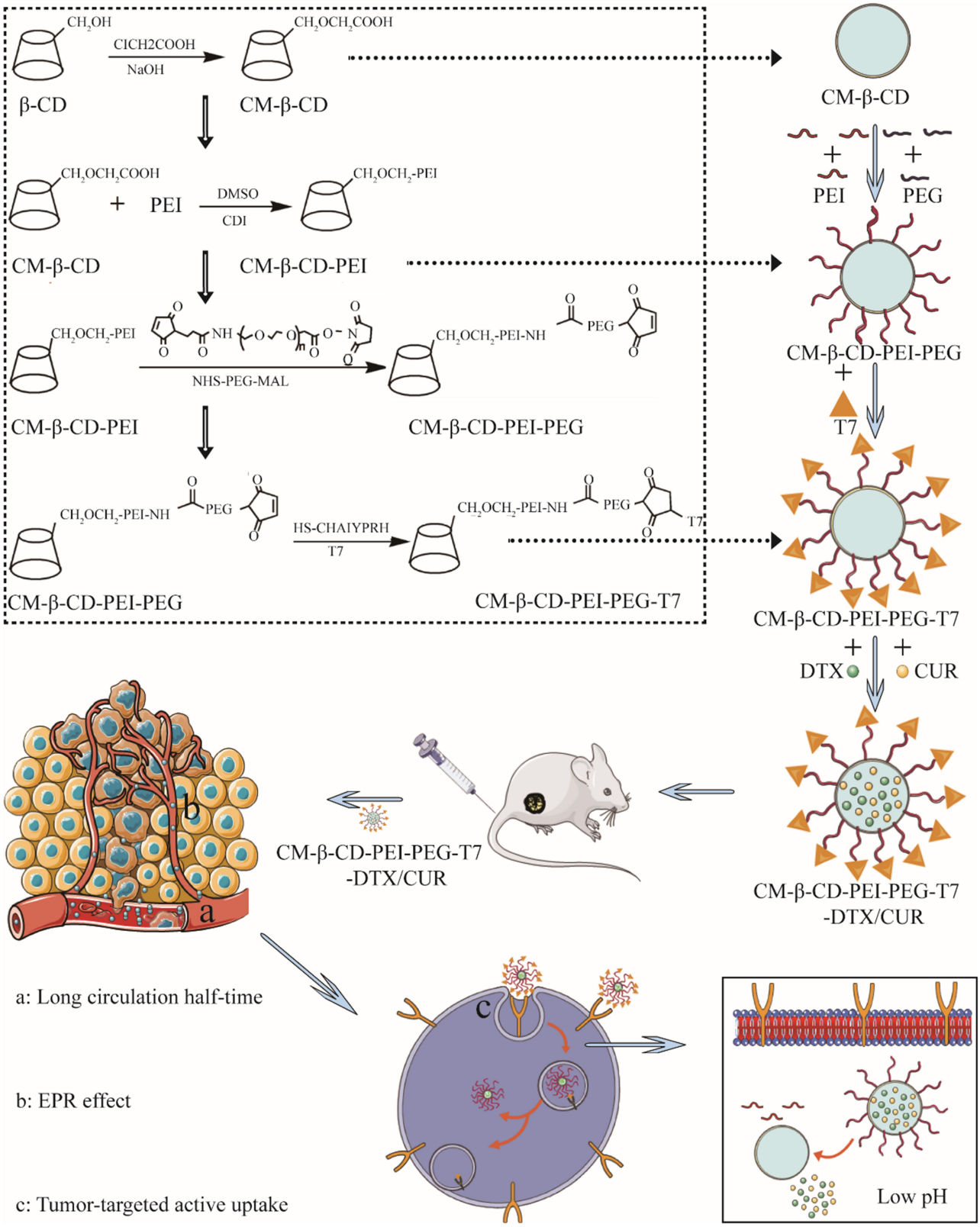

Scheme 1 Schematic diagram of the preparation of the CM-β-CD-PEI-PEG-T7 copolymer.

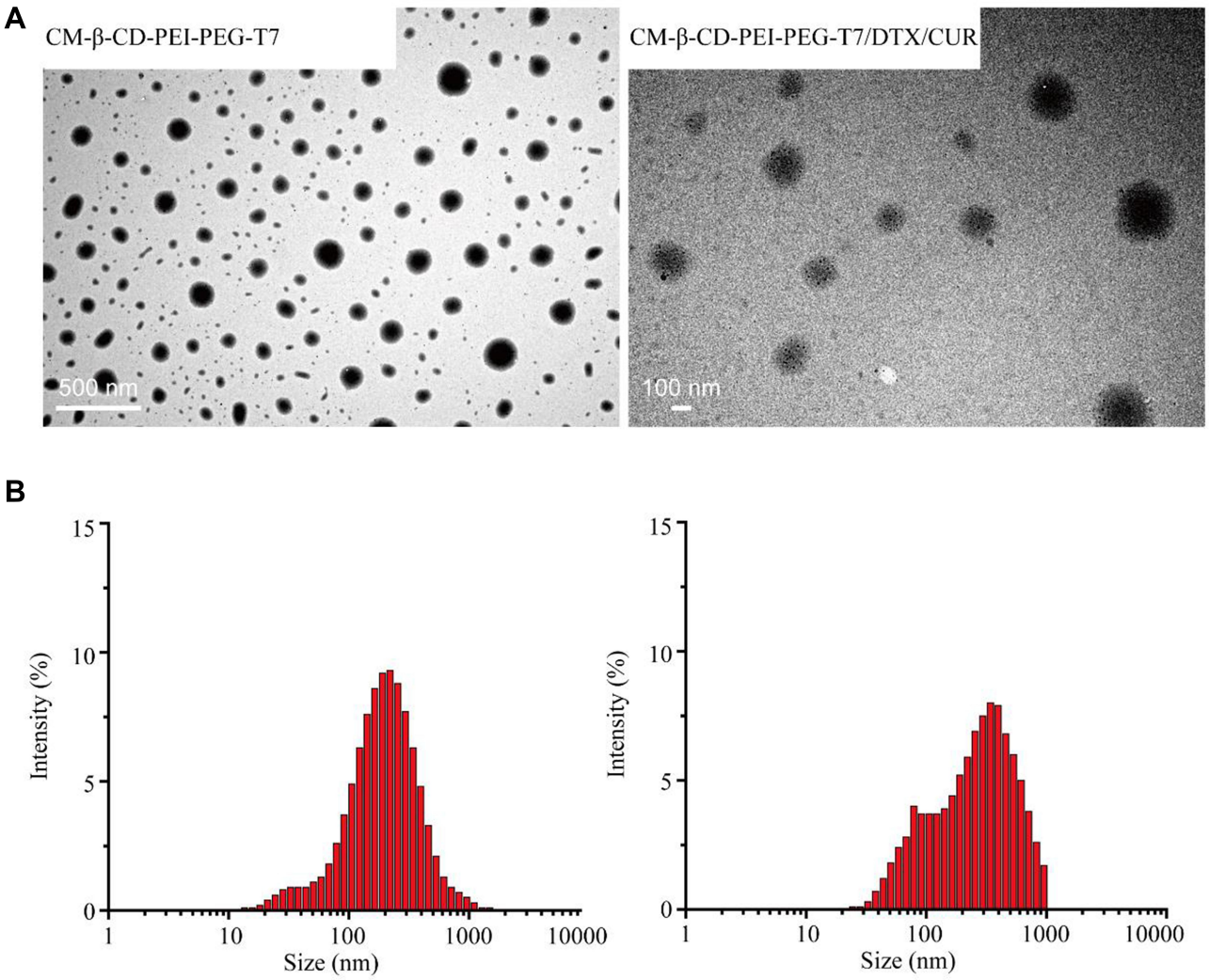

Figure 2 Characterization of nanoparticles. The size of nanoparticles (CM-β-CD-PEI-PEG-T7 and CM-β-CD-PEI-PEG-T7/DTX/CUR) was measured by TEM (**A**) and DLS (**B**).

cytometry (Figure 3A and B; Supplementary Figure S6A and S6B), and necrotic area by 3D tumorsphere experiment (Supplementary Figure S5A–B). At first, there was no damage observed after treatment with different concentrations of nanoparticles, indicating good biocompatibility (Supplementary Figure S4A–B). The IC_{50} values of the various nanomedicines, presented in Supplementary Table S2, indicated that the best anti-tumor effect was obtained by treatment with T7-NP-DC. Moreover, the anti-tumor efficacy of free docetaxel was enhanced by loading into the T7-NP. Similar results were obtained by flow cytometry and in the 3D tumorsphere experiment. Taking the results together, the nanocarrier has good biocompatibility and has confirmed drug-delivery capability. Co-delivery of curcumin could enhance the anti-tumor effect of docetaxel on esophageal cancer.

Cellular Uptake

The random distribution of drugs is a major obstacle to their anti-tumor effect.[34] When the therapeutic drug is loaded into a nanocarrier with a targeting effect, it will be equivalent to a smart bomb that can exert its killing-effect in specific parts of the body. Previously, numerous studies have confirmed that when the drug is loaded into a nanocarrier, significantly enhanced distribution to the tumor can be achieved, which not only increases the efficacy of free drugs, but also protects normal tissues from damage.[35] For this study, we developed a nanocarrier binding the TfR of the tumor surface.

The FITC-labeled nanoparticles were used to examine the targeting ability of T7-decorated nanoparticles to cells in vitro. Compared with the NP group, cellular

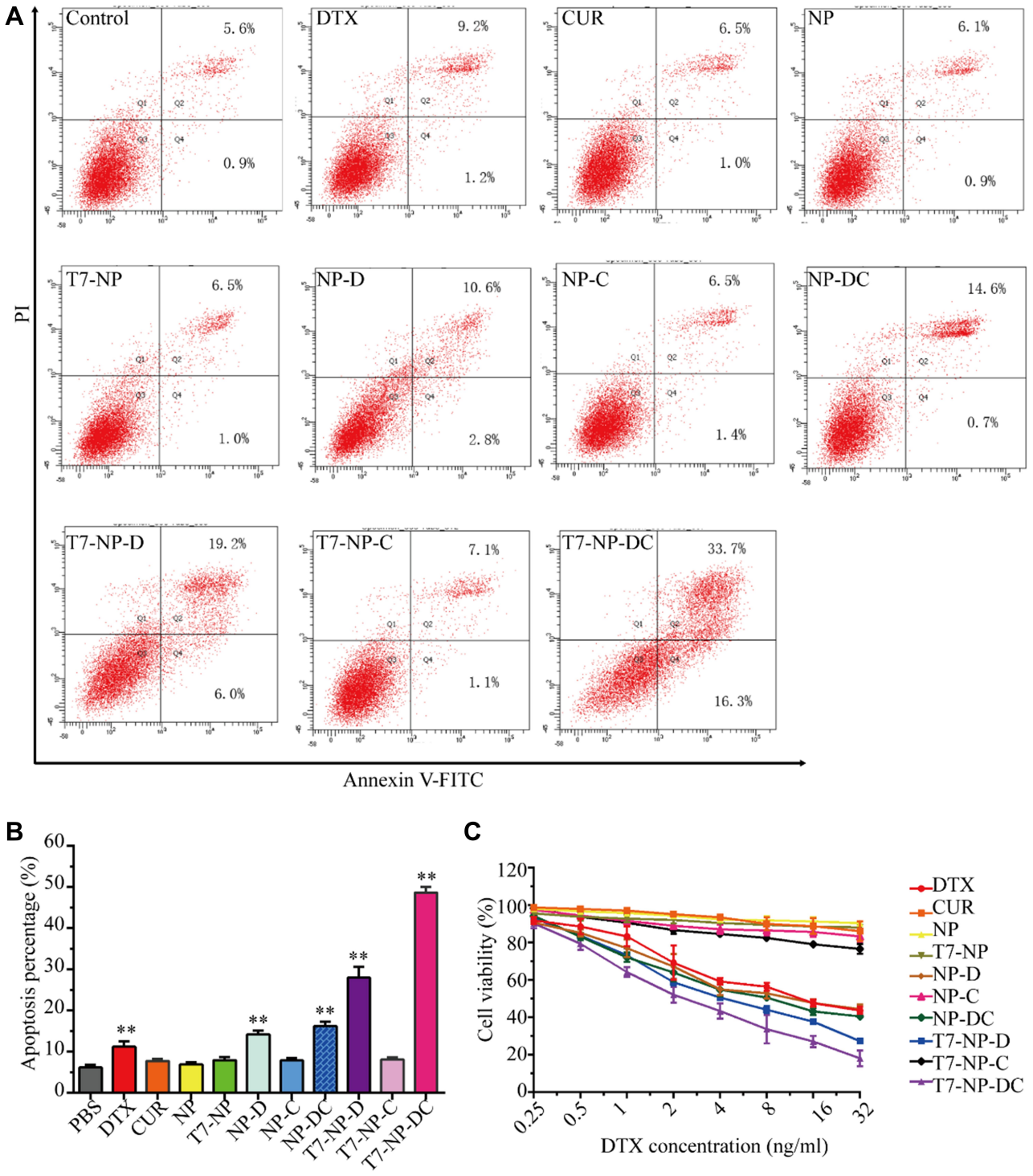

Figure 3 Synergistic anti-tumor efficacy of nanomedicines in ESCC. Cells (KYSE150) were incubated with different treatments (DTX, CUR, NP, T7-NP, NP-D, NP-C, NP-DC, T7-NP-D, T7-NP-C, and T7-NP-DC) for 48 hours. Cell viability was then determined by flow cytometry (**A, B**) and CCK-8 assay (**C**).** *P*<0.01.

uptake of T7-NP, with T7-modification, was greater and could be suppressed or promoted by the addition of free-T7 peptide and transferrin, respectively (Figure 4 and Supplementary Figure S7). Prior research has demonstrated that T7-conjugated lipid nanoparticles could enhance cellular uptake compared to non-targeted nanoparticles.[29] Recently, there has been another report demonstrating the better cellular uptake

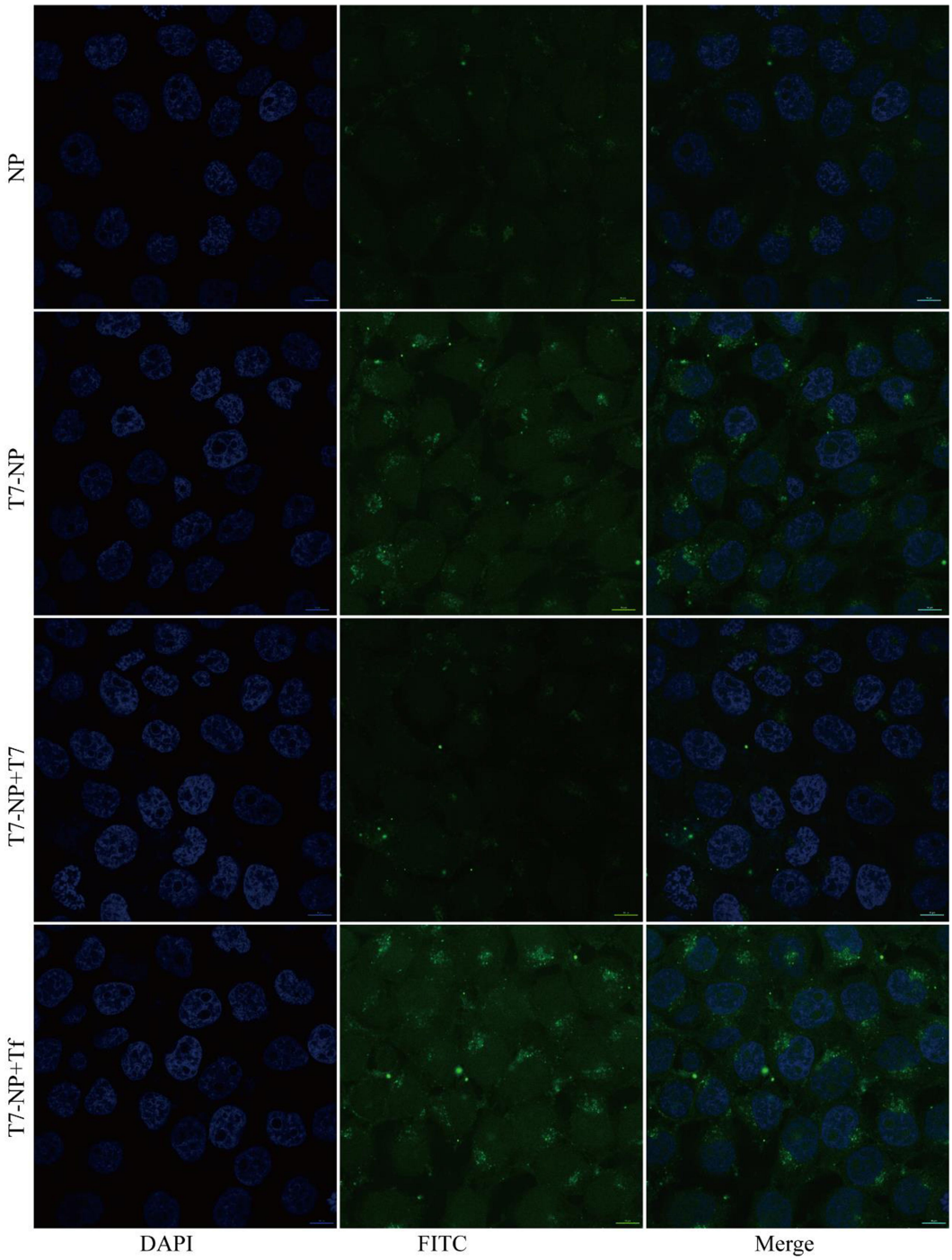

Figure 4 Preferential cellular uptake of T7-modified nanoparticles. Cells (KYSE150) in good condition were pretreated with FITC-labeled nanoparticles composed of different treatments. The fluorescence intensity in cells was then observed using a confocal microscope. Cellular uptake of T7-decorated nanoparticles was superior to that of nanoparticles without T7-decoration.

of T7-decorated exosomes compared with unmodified-exosomes in the treatment of glioblastoma.[36] These findings indicate that T7-modified nanoparticles could enhance the uptake efficiency of esophageal cancer cells.

Biodistribution of Nanoparticles in vivo

Tumor-bearing mice were divided into five groups (PBS, NP, NP-DC, T7-NP-D, and T7–NP–DC). Cy5.5-labeled nanoparticles were injected intravenously prior to in vivo imaging. After 2 hours there was no significant difference

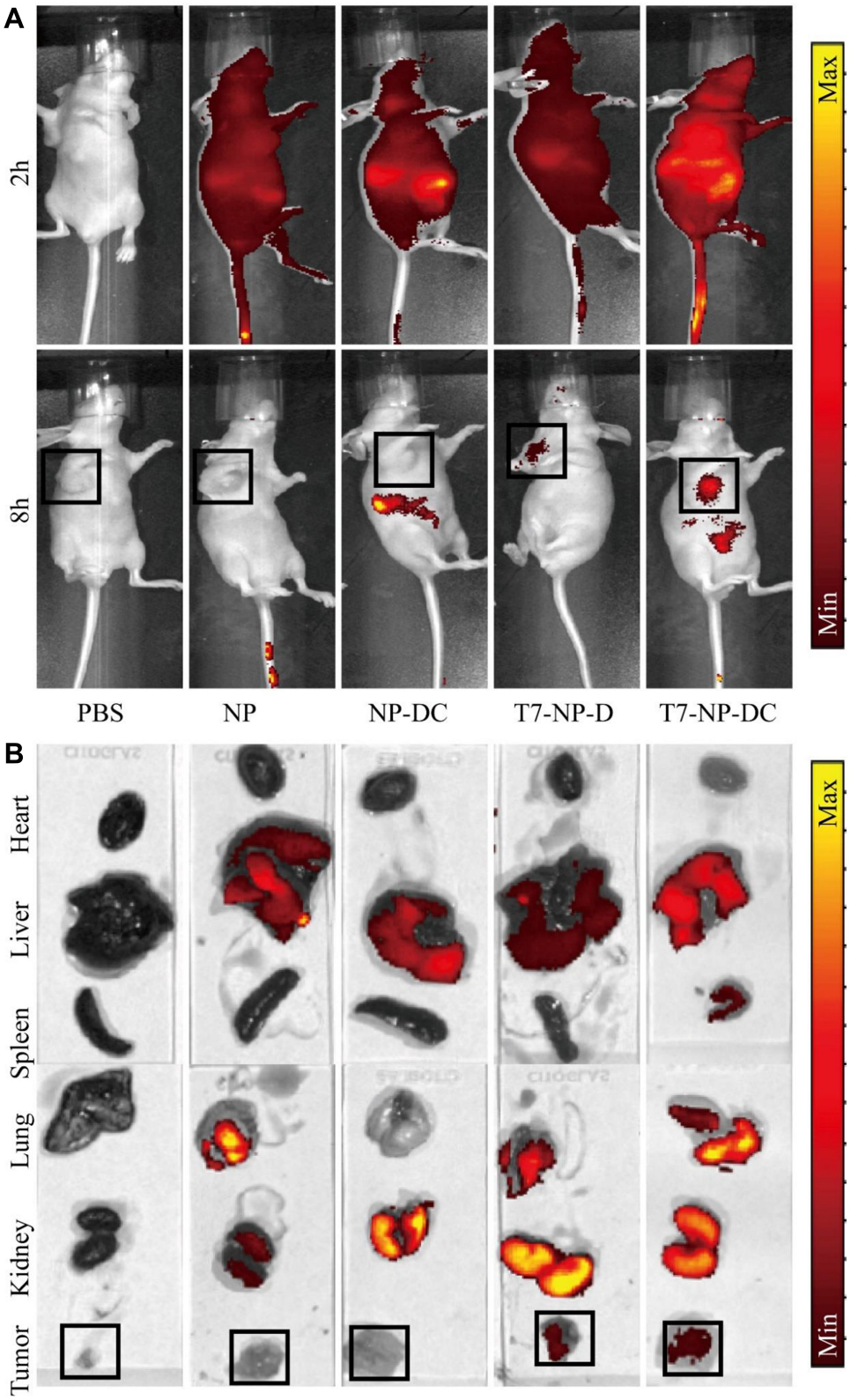

Figure 5 Biodistribution of nanocarriers in vivo. Tumor-bearing mice were divided into five groups (PBS, NP, NP-DC, NPT-D, and NPT-DC). After intravenous injection of Cy5.5-labeled nanoparticles, their enrichment in the body was explored using an IVIS Spectrum System (**A**) and the major organs were harvested and imaged (**B**).

among all groups. The Cy5.5-labeled nanoparticles were distributed throughout the body, especially in the liver and kidney (Figure 5A). Examination 8 hours post-injection, as shown in Figure 5A, showed greatly decreased fluorescence. Nanoparticles without T7-modification had been eliminated from the tumor, while those with the modification remained in the tumor site. Our results confirm previous studies showing that the enhanced permeability and retention (EPR) effect of the nanomaterial can be improved by coupling short peptides for surface targeting.[37] The major organs (kidney, liver, lung, spleen, and heart) and tumors were harvested after the mice had been euthanized, and then imaged as described earlier. The T7-NP-D and T7-NP-DC groups showed enrichment of Cy5.5-labeled nanoparticles in tumors. In the other two groups, no fluorescence was observed in the tumor tissue and only residual nanoparticles were seen in the liver and kidney (Figure 5B). A previous study confirmed that T7-conjugated nanoparticles could be co-internalized with receptor-bound transferrin.[38] In essence, nanoparticles with T7-modification have a good tumor targeting effect, indicating that the system is a good platform for delivery of anti-tumor drugs to tumor tissue.

Anti-Tumor Efficacy and Biosafety in vivo

As planned, tumor-bearing mice were divided into six groups (PBS, NP-D, NP-DC, T7-NP-D, T7-NP-DC), and tumor volumes were measured every other day until the end of treatment. At the end of the experiment, blood was collected and major organs (lung, heart, liver, kidney, and spleen) and tumors were harvested for HE staining and IHC analysis. As shown in Figure 6A and C, inhibitory activity was observed in all groups except the PBS group, indicating the efficacy of docetaxel toward the xenografts. Moreover, a better anti-tumor effect was seen in the T7-NP -D and T7-NP-DC groups than in the NP-D and NP-DC groups that lacked the T7-modification, suggesting that the enhancement of an anti-tumor effect was induced by decoration with the T7 targeting-peptide. Furthermore, the best inhibitory effect was obtained by the administration of T7-NP-DC according to the immunohistochemistry results (Figure 6D and E). In a study on melanoma, nanoparticles formed from PEG-b-PPS-b-PEI enhanced the anti-tumor effect without deleterious effects.[39] A previous study reported that nanoparticle co-delivery of docetaxel and curcumin could synergistically enhance activity against breast cancer cells.[12] Therefore, these in vivo results suggest that the combination of docetaxel and curcumin has synergistic anti-tumor efficacy.

The toxicity of the nanomedicines to blood and major organs was also investigated. After administration of the nanomedicines for 12 days, there was no weight loss and no deleterious effect on hematopoietic function among the treatment groups (Figure 6B and Supplementary S8). There was also no obvious damage observed in the major organs using HE staining (Figure 7).

Discussion

Although a lot of manpower and material resources have been invested in tumor research, the prognosis of cancer patients is still not optimistic. The most important issues are tumor recurrence and metastasis after development of drug resistance. Chemotherapy, as the main treatment of malignant tumors, still has further potential to be explored. Docetaxel, a commonly used chemotherapeutic drug in patients with advanced non-small cell lung cancer (NSCLC), has achieved remarkable results in the clinic. Recent research findings suggest that docetaxel alone can achieve overall survival of 10.5 months in patients with NSCLC[40]. However, effective cancer treatment is difficult to achieve with single chemotherapy, radiotherapy, and surgery,so combined treatment is currently highly favored. Although curcumin has not been used in the clinic, it has been demonstrated that curcumin has good chemosensitivity in ovarian and breast cancers.[41] Furthermore, it has been reported that curcumin can regulate proliferation of tumor cells by modulation of the PI3K/Akt and NF-kB signaling pathways.[42] It has been suggested that curcumin can kill liver tumor stem cells, which are the most important mediators of tumor recurrence and metastasis.[43] In the current study, we also found that a combination of curcumin with docetaxel significantly reduced the IC_{50} of docetaxel in the treatment of lung cancer cells compared to docetaxel alone. In addition, combined therapy inhibited growth of lung cancer cells in tumorspheres. These results suggest that curcumin combined with low dose docetaxel can not only improve the therapeutic effect in lung cancer, but also reduce adverse reactions caused by docetaxel, such as allergy, neutropenia, and other symptoms. Although the benefits of curcumin and docetaxel combination can be confirmed in vitro, the situation in vivo is more complex. When free drugs are used in vivo, the non-targeted distribution to normal tissues can lead to low concentrations in the tumor and, consequently, poor efficacy.

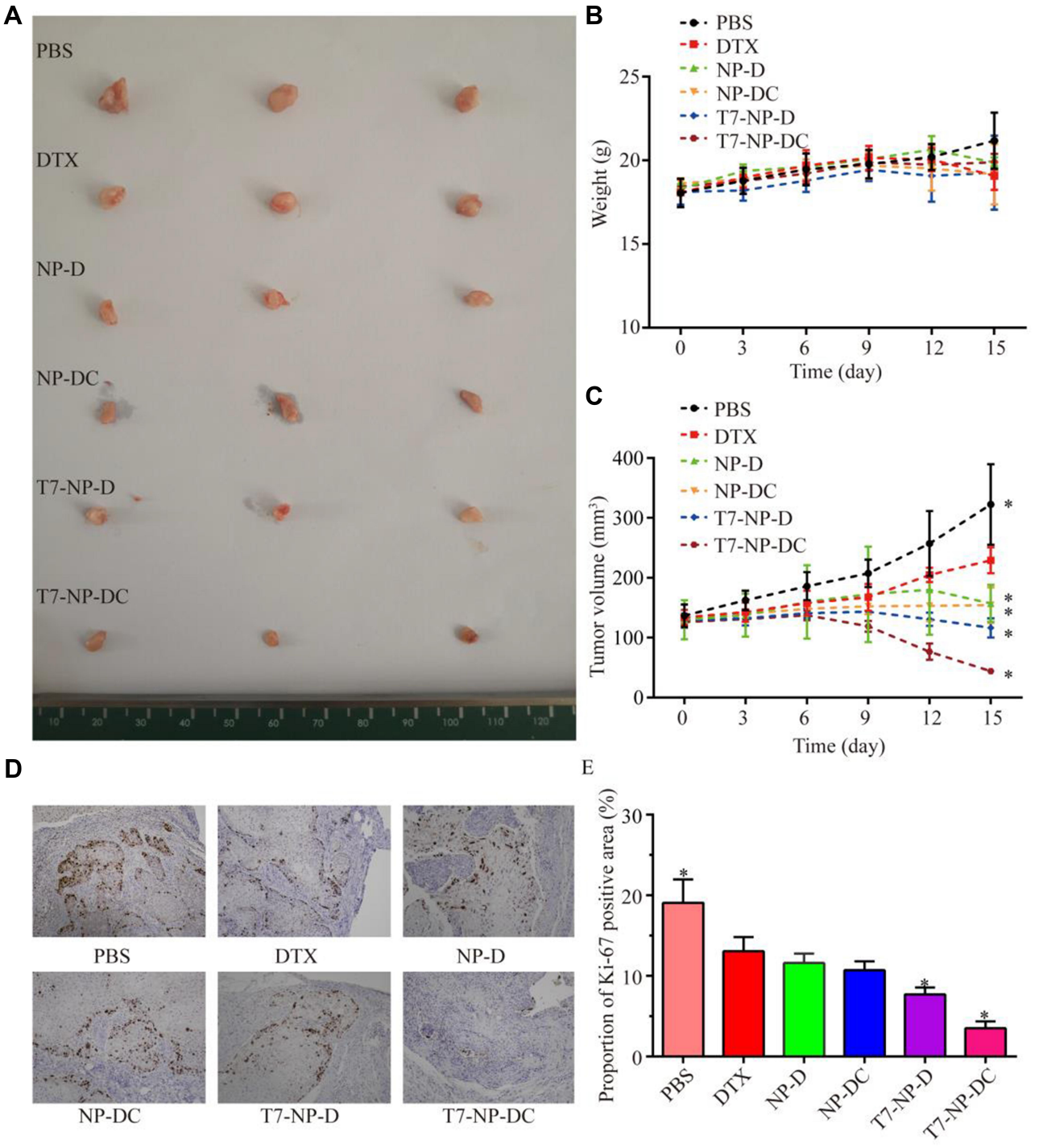

Figure 6 Anti-tumor efficacy in vivo. Tumor-bearing mice were divided into six groups (PBS, DTX, NP-DTX, NP-DTX/CUR, T7-NP-DTX, and T7-NP-DTX/CUR), treated by intravenous injection every other day for a total of 12 days. The mice were weighed (**B**) and tumors were harvested (**A**) and measured (**C**). Then, immunohistochemistry was conducted to investigate the expression of Ki-67 in response to various drug formulations (**D, E**). * $P<0.05$, ** $P<0.01$.

In recent years, nanomaterials have been widely explored because of their unique physical and chemical properties, such as: (1) long half-life in vivo; (2) tumor enrichment effect; (3) tumor environment responsive release.[44] Polyethylene glycol (PEG) is a hydrophilic polymer that has good water solubility. By increasing the molecular volume of a drug, it can effectively prolong the half-life of the drug in vivo. At the same time, it can mask immune sites on the drug to significantly reduce immunogenicity. Furthermore, it can avoid

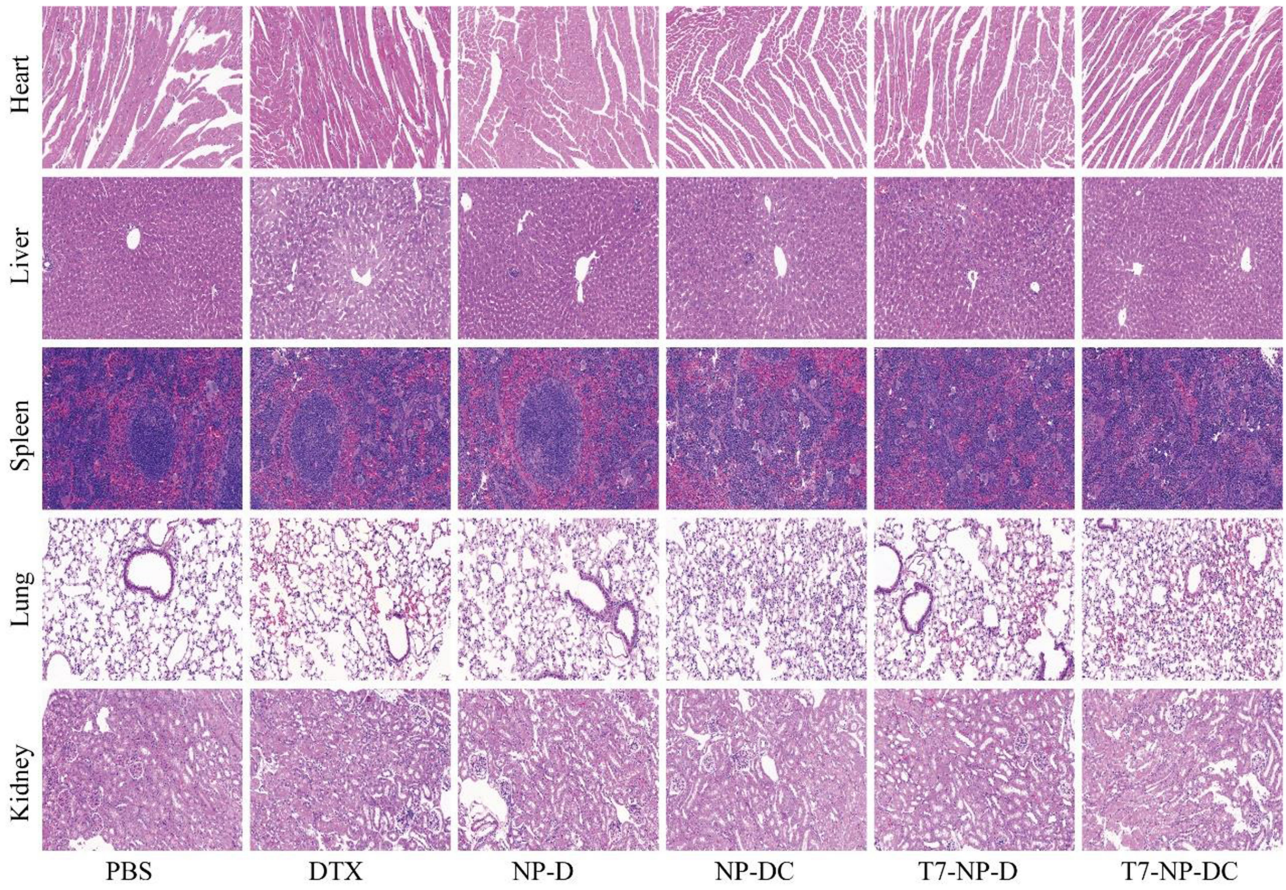

Figure 7 Biocompatibility of nanomedicines in vivo. There was no significant damage observed by HE staining of heart, liver, spleen, lung, or kidney after 12 days treatment with different nanomedicines.

recognition by the reticuloendothelial system, enhance blood circulation retention, and enhance accumulation in tumor tissue through the PR effect. Furthermore, polyethyleneimine (PEI) is a widely used cationic polymer that can assist entry of nanoparticles into tumor cells via their negatively charged cell membranes. We found that T7-NP modified with T7 could more easily enter tumor cells than NP both in vitro and in vivo. To a certain extent, tumor treatment depends on the concentration of therapeutic drug in the tumor environment. The nanomedicines we prepared not only increase the concentration of drugs in the tumor tissue to give a better therapeutic effect, but also exhibit improved biosafety compared to the free drugs. The prepared nanomedicine enhanced distribution to tumor tissue via T7 targeting, and then increased the concentrations of docetaxel and curcumin in the tumor by pH-responsive release to exert a synergistic antitumor effect. Some of the chemotherapeutics currently used in the clinic have an immunomodulatory effect in addition to a cytotoxic effect. For example, gemcitabine can selectively clear myeloid-derived suppressor cells (MDSC).[45] Doxorubicin can induce immunogenic death of tumor cells, releasing tumor antigens that activate antigen presentation by dendritic cells, and enhance the immune effect of T cells.[46] Paclitaxel and docetaxel are also considered to be inducers of cell immunogenic death.[47] However, the Balb/cnude mice used in this study are immunodeficient mice, so the results do not reflect any contributory effects of the nanomedicine on the tumor immune microenvironment.

In summary, we have successfully built a novel T7-targeting nanocarrier with pH-responsive drug-release capability. The targeting ability, anti-tumor activity, and biocompatibility of the system have been verified in vivo and in vitro. The nanomedicines not only have superior targeting ability, but also exhibit a synergistic anti-tumor effect. This study has laid a foundation for future development of combination-chemotherapy.

Abbreviations

CCK-8, cell counting kit-8; ^{1}H NMR, nuclear magnetic resonance spectroscopy; CLSM, confocal laser scanning microscope; TEM, transmission electron microscopy; DLS, dynamic light scattering; HE, hematoxylin-eosin; IHC, immunohistochemistry; CI, combination index; TfR, transferrin receptor; CDI, carbonyldiimidazole; DTX, docetaxel; CUR, curcumin; DMSO, dimethyl sulfoxide; PEI, polyethyleneimine; NHS-PEG-MAL, α-maleimidyl-ω-N-hydroxysuccinimidyl polyethylene glycol; β-CD, β-cyclodextrin; CM-β-CD, carboxymethylated β-CD; NP, CM-β-CD-PEI-PEG; T7-NP, CM-β-CD-PEI-PEG-T7; NP-D, CM-β-CD-PEI-PEG-DTX; NP-C, CM-β-CD-PEI-PEG-CUR; NP-DC, CM-β-CD-PEI-PEG-DTX/CUR; T7-NP-D: CM-β-CD-PEI-PEG-T7/DTX; T7-NP-C, CM-β-CD-PEI-PEG-T7/CUR; T7-NP-DC, CM-β-CD-PEI-PEG-T7/DTX/CUR.

Ethics Approval and Consent to Participate

All animal experiments were approved by the Southern Medical University Animal Care and Use Committee. The welfare of animal in vivo experiment is carried out in strict accordance with "Guidelines on kindly treatments for experimental animals" by the Science and Technology Ministry of the People's Republic of China (2006), 398.

Acknowledgments

The authors thank the cooperation of Beogene Biotechnology Company.

Funding

This work was supported by a grant from the National Natural Science Foundation of China (No. 81974434), a grant from the Natural Science Foundation of Guangdong Province (No. 2018A0303130233), grants from the Science and Technology of Guangdong Province (Nos. 2018A050506021, 2018A050506019, 2018A050506040), and grants from the Science and Technology Program of Guangzhou (Nos. 201907010037, 201907010032).

Disclosure

The authors declare no competing financial interest. The authors report no conflicts of interest for this work.

References

1. van Rossum PSN, Mohammad NH, Vleggaar FP, van Hillegersberg R. Treatment for unresectable or metastatic oesophageal cancer: current evidence and trends. *Nat Rev Gastroenterol Hepatol*. 2018;15(4):235–249.
2. Yamasaki M, Yasuda T, Yano M, et al. Multicenter randomized Phase II study of cisplatin and fluorouracil plus docetaxel (DCF) compared with cisplatin and fluorouracil plus Adriamycin (ACF) as preoperative chemotherapy for resectable esophageal squamous cell carcinoma (OGSG1003). *Ann Oncol*. 2017;28(1):116–120. doi:10.1093/annonc/mdw439
3. Ohashi S, Miyamoto S, Kikuchi O, Goto T, Amanuma Y, Muto M. Recent advances from basic and clinical studies of esophageal squamous cell carcinoma. *Gastroenterology*. 2015;149(7):1700–1715. doi:10.1053/j.gastro.2015.08.054
4. Rogers JE, Ajani JA. Taxane- versus cisplatin-based chemotherapy with radiation therapy is a better platform to refine esophageal cancer therapy. *J Clin Oncol*. 2019;37(30):2805. doi:10.1200/JCO.19.01247
5. Muro K, Hamaguchi T, Ohtsu A, et al. A phase II study of single-agent docetaxel in patients with metastatic esophageal cancer. *Ann Oncol*. 2004;15(6):955–959. doi:10.1093/annonc/mdh231
6. Lockhart AC, Reed CE, Decker PA, et al. Phase II study of neoadjuvant therapy with docetaxel, cisplatin, panitumumab, and radiation therapy followed by surgery in patients with locally advanced adenocarcinoma of the distal esophagus (ACOSOG Z4051) (vol 25, pg 1039, 2014). *Ann Oncol*. 2019;30(2):345.
7. Mitra K, Gautam S, Kondaiah P, Chakravarty AR. The cis-diammineplatinum(II) complex of curcumin: a dual action DNA crosslinking and photochemotherapeutic agent (vol 54, pg 13989, 2015). *Angew Chem Int Ed*. 2019;58(44):15576. doi:10.1002/anie.201910812
8. Nelson KM, Dahlin JL, Bisson J, Graham J, Pauli GF, Walters MA. The essential medicinal chemistry of curcumin. *J Med Chem*. 2017;60(5):1620–1637. doi:10.1021/acs.jmedchem.6b00975
9. Bayet-Robert M, Kwiatkowski F, Leheurteur M, et al. Phase I dose escalation trial of docetaxel plus curcumin in patients with advanced and metastatic breast cancer. *Cancer Biol Ther*. 2010;9(1):8–14. doi:10.4161/cbt.9.1.10392
10. Lin YG, Kunnumakkara AB, Nair A, et al. Curcumin inhibits tumor growth and angiogenesis in ovarian carcinoma by targeting the nuclear factor-kappa B pathway. *Clin Cancer Res*. 2007;13(11):3423–3430. doi:10.1158/1078-0432.CCR-06-3072
11. Yan JK, Wang YZ, Jia YX, et al. Co-delivery of docetaxel and curcumin prodrug via dual-targeted nanoparticles with synergistic antitumor activity against prostate cancer. *Biomed Pharmacother*. 2017;88:374–383. doi:10.1016/j.biopha.2016.12.138
12. Sahu BP, Hazarika H, Bharadwaj R, et al. Curcumin-docetaxel co-loaded nanosuspension for enhanced anti-breast cancer activity. *Expert Opin Drug Deliv*. 2016;13(8):1065–1074. doi:10.1080/17425247.2016.1182486
13. Chow EKH, Ho D. Cancer nanomedicine: from drug delivery to imaging. *Sci Transl Med*. 2013;5(216).
14. Yu GC, Yu S, Saha ML, et al. A discrete organoplatinum(II) metallacage as a multimodality theranostic platform for cancer photochemotherapy. *Nat Commun*. 2018;9.
15. Zhu HTZ, Wang HH, Shi BB, et al. Supramolecular peptide constructed by molecular Lego allowing programmable self-assembly for photodynamic therapy. *Nat Commun*. 2019;10.
16. Ma ZR, Wan H, Wang WZ, et al. A theranostic agent for cancer therapy and imaging in the second near-infrared window. *Nano Res*. 2019;12(2):273–279. doi:10.1007/s12274-018-2210-x
17. Zhao H, Xu J, Li Y, et al. Nanoscale coordination polymer based nanovaccine for tumor immunotherapy. *Acs Nano*. 2019;13(11):13127–13135. doi:10.1021/acsnano.9b05974

18. Yin JY, Lang TQ, Cun DM, et al. pH-sensitive nano-complexes overcome drug resistance and inhibit metastasis of breast cancer by silencing Akt expression. *Theranostics*. 2017;7(17):4204–4216.
19. Mura S, Nicolas J, Couvreur P. Stimuli-responsive nanocarriers for drug delivery. *Nat Mater*. 2013;12(11):991–1003.
20. Jiang K, Chi T, Li T, et al. A smart pH-responsive nano-carrier as a drug delivery system for the targeted delivery of ursolic acid: suppresses cancer growth and metastasis by modulating P53/MMP-9/PTEN/CD44 mediated multiple signaling pathways. *Nanoscale*. 2017;9(27):9428–9439. doi:10.1039/C7NR01677H
21. Li YF, Chen M, Yao BW, et al. Transferrin receptor-targeted redox/pH-sensitive podophyllotoxin prodrug micelles for multidrug-resistant breast cancer therapy. *J Mater Chem B*. 2019;7(38):5814–5824.
22. Moreira AF, Dias DR, Costa EC, Correia IJ. Thermo- and pH-responsive nano-in-micro particles for combinatorial drug delivery to cancer cells. *Eur J Pharm Sci*. 2017;104:42–51. doi:10.1016/j.ejps.2017.03.033
23. Yu MA, Su DY, Yang YY, et al. D-T7 peptide-modified PEGylated bilirubin nanoparticles loaded with cediranib and paclitaxel for anti-angiogenesis and chemotherapy of glioma. *Acs Appl Mater Inter*. 2019;11(1):176–186. doi:10.1021/acsami.8b16219
24. Bi YK, Liu LS, Lu YF, et al. T7 peptide-functionalized PEG-PLGA micelles loaded with carmustine for targeting therapy of glioma. *Acs Appl Mater Inter*. 2016;8(41):27465–27473. doi:10.1021/acsami.6b05572
25. Talelli M, Barz M, Rijcken CJF, Kiessling F, Hennink WE, Lammers T. Core-crosslinked polymeric micelles: principles, preparation, biomedical applications and clinical translation. *Nano Today*. 2015;10(1):93–117. doi:10.1016/j.nantod.2015.01.005
26. Wang Q, Zeng F, Sun Y, et al. Etk interaction with PFKFB4 modulates chemoresistance of small-cell lung cancer by regulating autophagy. *Clin Cancer Res*. 2018;24(4):950–962. doi:10.1158/1078-0432.CCR-17-1475
27. Shen Y, Li X, Dong DD, Zhang B, Xue YR, Shang P. Transferrin receptor 1 in cancer: a new sight for cancer therapy. *Am J Cancer Res*. 2018;8(6):916–931.
28. Shao ZY, Shao JY, Tan BX, et al. Targeted lung cancer therapy: preparation and optimization of transferrin-decorated nanostructured lipid carriers as novel nanomedicine for co-delivery of anticancer drugs and DNA. *Int J Nanomed*. 2015;10.
29. Cheng XW, Yu DR, Cheng G, et al. T7 peptide-conjugated lipid nanoparticles for dual modulATION of Bcl-2 and Akt-1 in lung and cervical carcinomas. *Mol Pharmaceut*. 2018;15(10):4722–4732. doi:10.1021/acs.molpharmaceut.8b00696
30. Nag M, Gajbhiye V, Kesharwani P, Jain NK. Transferrin functionalized chitosan-PEG nanoparticles for targeted delivery of paclitaxel to cancer cells. *Colloids Surf B*. 2016;148:363–370. doi:10.1016/j.colsurfb.2016.08.059
31. Yu MX, Zheng J. Clearance pathways and tumor targeting of imaging nanoparticles. *Acs Nano*. 2015;9(7):6655–6674. doi:10.1021/acsnano.5b01320
32. Zhang YJ, Takahashi Y, Hong SP, et al. High-resolution label-free 3D mapping of extracellular pH of single living cells. *Nat Commun*. 2019;571(7766):10. doi:10.1038/s41586-019-1351-8
33. Mikhail AS, Allen C. Poly(ethylene glycol)-b-poly(epsilon-caprolactone) micelles containing chemically conjugated and physically entrapped docetaxel: synthesis, characterization, and the influence of the drug on micelle morphology. *Biomacromolecules*. 2010;11(5):1273–1280.
34. Song GS, Cheng L, Chao Y, Yang K, Liu Z. Emerging nanotechnology and advanced materials for cancer radiation therapy. *Adv Mater*. 2017;29(32).
35. Lang TQ, Liu YR, Zheng Z, et al. Cocktail strategy based on spatio-temporally controlled nano device improves therapy of breast cancer (vol 31, 1806202, 2019). *Adv Mater*. 2019;31:33.
36. Kim G, Kim M, Lee Y, Byun JW, Hwang DW, Lee M. Systemic delivery of microRNA-21 antisense oligonucleotides to the brain using T7-peptide decorated exosomes. *J Control Release*. 2019;317:273–281. doi:10.1016/j.jconrel.2019.11.009
37. Jia G, Han Y, An YL, et al. NRP-1 targeted and cargo-loaded exosomes facilitate simultaneous imaging and therapy of glioma in vitro and in vivo. *Biomaterials*. 2018;178:302–316. doi:10.1016/j.biomaterials.2018.06.029
38. Oh S, Kim BJ, Singh NP, Lai H, Sasaki T. Synthesis and anti-cancer activity of covalent conjugates of artemisinin and a transferrin-receptor targeting peptide. *Cancer Lett*. 2009;274(1):33–39. doi:10.1016/j.canlet.2008.08.031
39. Velluto D, Thomas SN, Simeoni E, Swartz MA, Hubbell JA. PEG-b-PPS-b-PEI micelles and PEG-b-PPS/PEG-b-PPS-b-PEI mixed micelles as non-viral vectors for plasmid DNA: tumor immunotoxicity in B16F10 melanoma. *Biomaterials*. 2011;32(36):9839–9847. doi:10.1016/j.biomaterials.2011.08.079
40. Pillai RN, Fennell DA, Kovcin V, et al. Randomized phase III study of ganetespib, a heat shock protein 90 inhibitor, with docetaxel versus docetaxel in advanced non-small-cell lung cancer (GALAXY-2). *J Clin Oncol*. 2020;38(6):613–622. doi:10.1200/JCO.19.00816
41. Chirnomas D, Taniguchi T, de la Vega M, et al. Chemosensitization to cisplatin by inhibitors of the Fanconi anemia/BRCA pathway. *Mol Cancer Ther*. 2006;5(4):952–961. doi:10.1158/1535-7163.MCT-05-0493
42. Fu H, Wang C, Yang D, et al. Curcumin regulates proliferation, autophagy, and apoptosis in gastric cancer cells by affecting PI3K and P53 signaling. *J Cell Physiol*. 2018;233(6):4634–4642. doi:10.1002/jcp.26190
43. Marquardt JU, Gomez-Quiroz L, Arreguin Camacho LO, et al. Curcumin effectively inhibits oncogenic NF-kappaB signaling and restrains stemness features in liver cancer. *J Hepatol*. 2015;63(3):661–669. doi:10.1016/j.jhep.2015.04.018
44. Shi J, Kantoff PW, Wooster R, Farokhzad OC. Cancer nanomedicine: progress, challenges and opportunities. *Nat Rev Cancer*. 2017;17(1):20–37.
45. Sasso MS, Lollo G, Pitorre M, et al. Low dose gemcitabine-loaded lipid nanocapsules target monocytic myeloid-derived suppressor cells and potentiate cancer immunotherapy. *Biomaterials*. 2016;96:47–62. doi:10.1016/j.biomaterials.2016.04.010
46. Yang W, Zhu G, Wang S, et al. In situ dendritic cell vaccine for effective cancer immunotherapy. *ACS Nano*. 2019;13(3):3083–3094. doi:10.1021/acsnano.8b08346
47. Qiao H, Chen X, Chen E, et al. Folated pH-degradable nanogels for the simultaneous delivery of docetaxel and an IDO1-inhibitor in enhancing cancer chemo-immunotherapy. *Biomater Sci*. 2019;7(7):2749–2758. doi:10.1039/C9BM00324J